JOURNAL OF PROPULSION AND POWER
Vol. 18, No. 6, November–December 2002

Comparison of Laser- and Pressure-Driven Thrust Response of HMX

Gautam N. Kudva* and Thomas A. Litzinger†
Pennsylvania State University, University Park, PA 16802

The laser- and pressure-driven thrust response functions of HMX (cyclotetramethylene tetranitramine) at pressures near 1 atm were measured during laser-supported combustion at mean CO_2 laser heat fluxes of 35 and 60 W/cm^2. During laser-driven testing, the laser flux was modulated at ± 15 W/cm^2 at driving frequencies ranging from 4 to 250 Hz. Pressure-driven thrust measurements were made with a 10% peak-to-peak variation about the mean chamber pressure at driving frequencies ranging from 4 to 100 Hz. Measured steady-state temperature profiles and numerical predictions of the temperature profiles in the gas-phase reaction zone were used to estimate steady and unsteady heat feedback, respectively. Trends in the experimental results are consistent with a condensed-phase response to the unsteady heat fluxes and with results in the literature from similar experiments. Differences in trends with changing mean heat flux between the laser- and pressure-driven results are explained using the unsteady heat feedback estimates. The experimental results are compared to an analytical model, which used one-step reactions in the condensed phase and gas phase, and numerical modeling results that used detailed gas-phase chemistry. The agreement between the analytical model and the data was found to be better than that between the numerical modeling results and the data.

Nomenclature

b	=	constant in regression rate law
f	=	frequency
M	=	molecular mass
m	=	burning rate per unit area
p	=	pressure
q	=	laser flux
R	=	universal gas constant
R_p	=	pressure-driven response function
R_q	=	radiation- (laser-) driven response function
r_b	=	surface regression rate
T_f	=	flame temperature
t_c	=	thermal relaxation time
$\bar{x}$	=	steady value of x
α	=	thermal diffusivity
Δx	=	oscillating value of x
ρ_c	=	density of condensed phase
ρ_g	=	density of gas phase
τ	=	thrust per unit area
Ω	=	nondimensional frequency
ω	=	angular frequency

Introduction

OSCILLATORY combustion in rocket motors was first measured in the 1940s with the advent of high-frequency pressure transducers. Large variations in the mean pressure and the resultant explosions of rocket motors made clear the need for solutions to oscillatory combustion. This increased awareness of oscillatory combustion formed the foundation for quantitative understanding of the phenomena that cause it. Typically, oscillations in the motor are sustained by a power input of less than 0.01% of the energy released during combustion, with the dynamic response of the combustion zone to flow disturbances and the damping processes in the combustor being the controlling parameters.

Until the 1960s, oscillatory combustion was avoided by geometrical changes to the rocket motor coupled with full-scale evaluations. Because of the increased cost of full-scale testing over the last 40 years, various research groups have focused on experimental, analytical, and numerical approaches to understand the problems associated with combustion instability. Devices such as T burners have been used to obtain a pressure oscillatory response function and admittance.[1,2] T burners have provided a tremendous amount of useful data and insight into combustion instability issues, but are relatively expensive to run and are unable to provide quantitative predictions for full-scale motors.

Several research groups have used radiation-driven experimental setups to study combustion instability, for example, see Refs. 3–7. The prime motivation behind these radiation-driven experiments is the belief that the radiation- (laser-) driven and pressure-driven experiments are closely related and that the radiation-driven response can be used to predict the pressure-driven response. The ease with which the laser can be modulated in frequency and power results in a controlled input source and allows for a relatively accurate response measurement.

Theoretical studies of laser-driven combustion instability have shown that the greater the transparency of a given propellant, the lower is the sensitivity of its condensed phase to the fluctuating radiant flux amplitude. This relationship is not present in pressure-driven combustion.[8] Hence, the laser- and pressure-driven response experiments cannot be considered to be analogous for propellants with high transparency. However, for opaque propellants, the normalized, linear response functions for laser- and pressure-driven combustion are predicted to be identical for small values of the average external radiant laser flux.[8] The theoretical models of Son and Brewster[9] for the linear pressure- and radiation-driven response of homogeneous materials relaxed the restriction of small values of average external radiative flux and showed that a constant scaling factor is inadequate to describe the relationship between the two response functions.

Two research groups have investigated the response of nitramine propellants in some detail. Extensive research has been done on HMX. Isbell and Brewster[10] determined the absorption coefficient of HMX at room temperature to be 5670 cm^{-1} for 10.6-μm radiation of CO_2 lasers, a parameter required for modeling in-depth absorption

Received 3 December 2001; revision received 29 August 2002; accepted for publication 4 September 2002.

*Research Assistant, Department of Mechanical and Nuclear Engineering; currently Process Engineer, Engineering, Corning Asahi, State College, PA 16801.

†Professor, Department of Mechanical and Nuclear Engineering. Member AIAA.

of laser energy. Loner and Brewster developed an analytical model of the oscillatory laser-augmented response of HMX, using one-step reactions in the condensed and gas phases and obtained experimental results to verify their predicted response function.[11] Brewster presented experimental results and modeling of HMX response functions that summarize the quasi-steady theory of solid propellant combustion response.[12] Other researchers to expend considerable effort on modeling the response of nitramine monopropellants were Erikson and Beckstead.[13] They developed a numerical model with detailed gas-phase kinetics that predicts both laser- and pressure-driven thrust response for RDX and HMX.

The primary objectives of the present study were to obtain laser- and pressure-driven thrust response data for nitramines under similar experimental conditions and to compare the pressure- and laser-driven responses. A secondary objective was to compare these results with the predictions of existing analytical and numerical models, namely, those by Loner and Brewster[11] and Erikson and Beckstead.[13] Unfortunately, the experimental thrust response data for RDX (cyclotrimethylene trinitramine) showed very small magnitudes during laser- and pressure-driven combustion, and so consistent data could not be obtained. Thus, the study focused on HMX.

Experimental Approach

Experiments for laser- and pressure-driven combustion of HMX were conducted at 1 atm with air as the ambient gas. (Thermocouple measurements confirmed that heat feedback from the final flame was not important for the conditions of this study so that the use of air, as opposed to an inert ambient gas, was expected to have little impact on the results.) HMX powder was pressed into 9.5-mm-diam pellets, which provided an adequate signal-to-noise ratio in the thrust signal. The pellets were tested in a quartz vial to eliminate side-burning effects so that the measured thrust was due to one-dimensional deflagration of the propellant sample. High-magnification video images were recorded using a Pulnix camera with a Nikon macrolens and a Mitsubishi video cassette recorder. Separate test chambers and procedures were used for laser- and pressure-driven combustion experiments. Detailed descriptions and features of the experimental setup have been described elsewhere,[14–18] and only a brief explanation will be given here.

Laser-Driven Experiments

Figure 1 shows a schematic of the experimental setup, including the triple-quadrupole mass spectrometer (TQMS), which has been used in past studies to measure species oscillations.[17] A Synrad 57-2 CO_2 laser was used as a heating source to ignite the propellant and sustain burning, as well as to generate the oscillatory heat flux. The laser beam had a Gaussian energy distribution and was passed through an expansion lens to give a nearly uniform heat flux, with a variation of 10% about the mean. The laser was combined with a visible diode beam for alignment. An Hewlett Packard-3245A universal source created the input signal to modulate the laser output, which was a series of sinusoidal frequencies for a single test. The laser beam passed through a beam splitter before entering the combustion chamber through a potassium chloride window. The beam splitter reflected 99.5% of the CO_2 laser power into the test chamber. The remaining 0.5% was focused onto an HgCdTe detector, which was used to monitor the laser waveform as a function of frequency. The chamber is 28 cm in height and has a volume of 8138 cm^3. Several holes of 9.5 mm diam were drilled into the bottom of

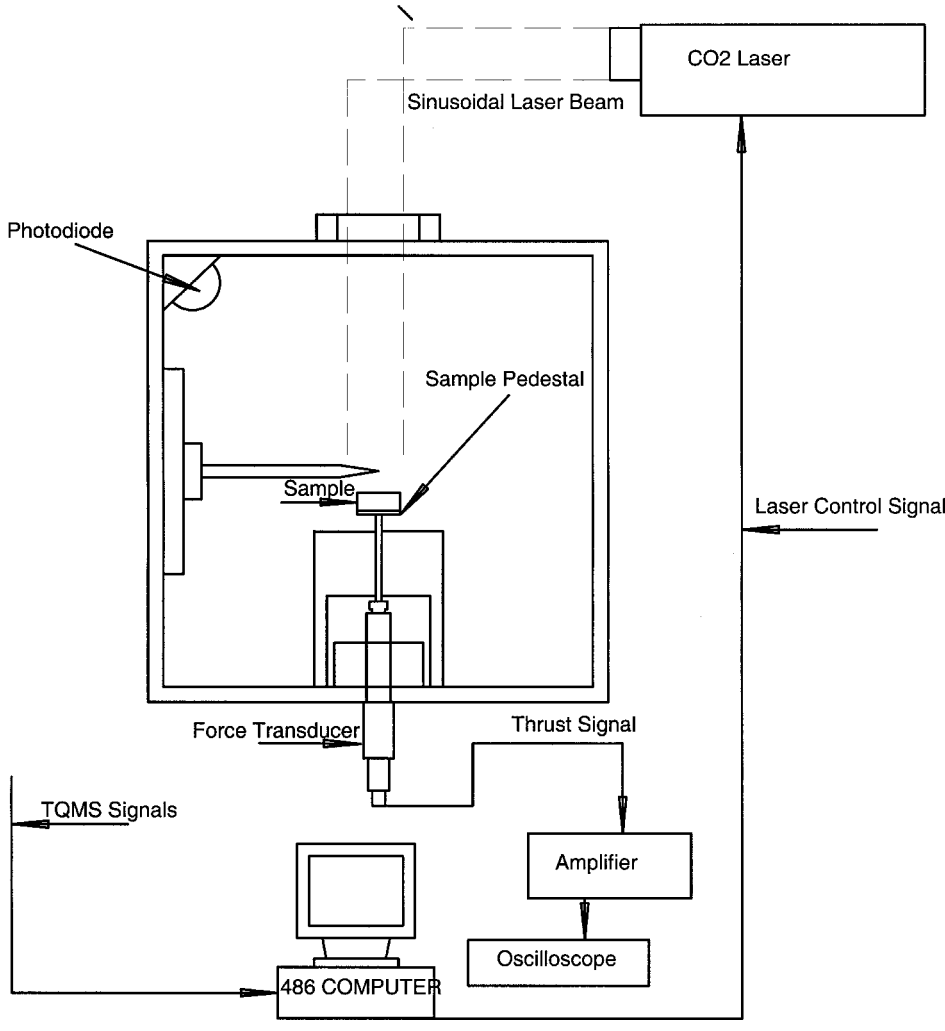

Fig. 1 Schematic of experimental setup for laser-driven combustion.

the chamber, and a mechanical pump was connected to the top of the chamber to remove the combustion gases continuously and to maintain atmospheric pressure.

Thrust was measured using a Kistler 9207 high-sensitivity microforce transducer. The transducer was placed in an aluminum block, which acted as a shield and prevented side loads. The natural frequency of the transducer on its test stand was determined to be approximately 10 kHz by imposing force impulses on the system, and all tests were performed below 1 kHz to minimize the effect of resonance on thrust measurements. The signal was amplified using a Kistler 5010 charge amplifier. A 1-kHz low-pass filter was used to remove unwanted high-frequency noise. Real-time experimental control of the CO_2 laser and data acquisition were performed through a computer program. The program allowed the user to input different frequencies and mean heat fluxes for a single test. The excitation signal and thrust were recorded on a two-channel digital oscilloscope whereas any additional signals were recorded on a personal computer with a data acquisition card and software. The data on the oscilloscope were stored on a floppy disc. VU-Point software from Nicolet was used to convert the data into text format. These text-formatted data were then converted into an EXCEL spreadsheet. A fast Fourier transform was performed on the thrust and excitation signals, and the ratio of the amplitudes of the thrust and laser heat flux variations was calculated to obtain the dimensional thrust response.

Pressure-Driven Experiments

Figure 2 presents the overall experimental setup for the pressure-driven thrust measurements. The CO_2 laser was used to ignite and sustain combustion of the propellant sample. The samples were also glued into a quartz vial to ensure that no side burn occurred, so that thrust for one-dimensional combustion was measured. The samples were placed perpendicular to the laser beam on a sample holder. A Cooper Instruments, pressure insensitive, LPM 510 subminiature load cell was used to measure thrust response. The load cell used a cantilever beam strain gauge mechanism and had a measured natural frequency of 800 Hz. The excitation energy for the load cell was provided by a 5-V dc power source. To prevent the load cell from being exposed to high-temperature gases, it was placed in a ceramic thermal shield. Testing of the complete test setup showed no resonance peaks below 400 Hz.

A pressure-driven combustion system that provides a nearly sinusoidal pressure variation was designed and built in-house.[16] Two model airplane engines are attached to opposite sides of the chamber and produce a peak-to-peak pressure variation of 10% of the mean, regardless of the chamber pressure and frequency of operation. The length of the chamber walls was 9 cm, and the chamber had a volume of 733 cm^3. To minimize the effects of velocity oscillations on the combustion response, the airplane engines were operated 180 deg out of phase, and the sample was placed in the middle of the chamber. Model BGX-1 airplane engines from O.S. Engine Company with a maximum operating frequency of 165 Hz were used. A 5-hp motor from Grainger, Inc., was used to drive the airplane engines through a drive belt and pulleys. An ac inverter, also from Grainger, Inc., supplied variable speeds to the motor by changing the input voltage frequency from 0 to 60 Hz. Variable speeds to the motor resulted in different piston velocities and, hence, changed the frequency of pressure oscillation within the combustion chamber. The motor and the test chamber were fixed to a rigid I-beam frame to reduce the engine and motor vibrations. The motor was mounted on an adjustable stand because different gears and drive belts were required to achieve the desired frequency range.

The small chamber volume resulted in a significant increase in mean pressure during combustion. To negate the effects of pressure increase within the combustion chamber on the load cell, the pressure insensitive load cell had a vent hole drilled along its bottom surface. In addition, an access path was created in the ceramic shield, which resulted in the ambient pressure being applied simultaneously to the top and bottom of the sensing element of the load cell. The leads from the load cell were connected to a differential amplifier (Ectron Model 428) through twisted-pair, insulated cables. The insulated cables prevented the radio frequency power source for the CO_2 laser power supply from contaminating the signal. Because of the small output from the load cell, an amplification of 500 was used to measure the thrust. The thrust signals were recorded on the Nicolet 310 digital oscilloscope whereas the photodiode signals were recorded on the secondary data acquisition system.

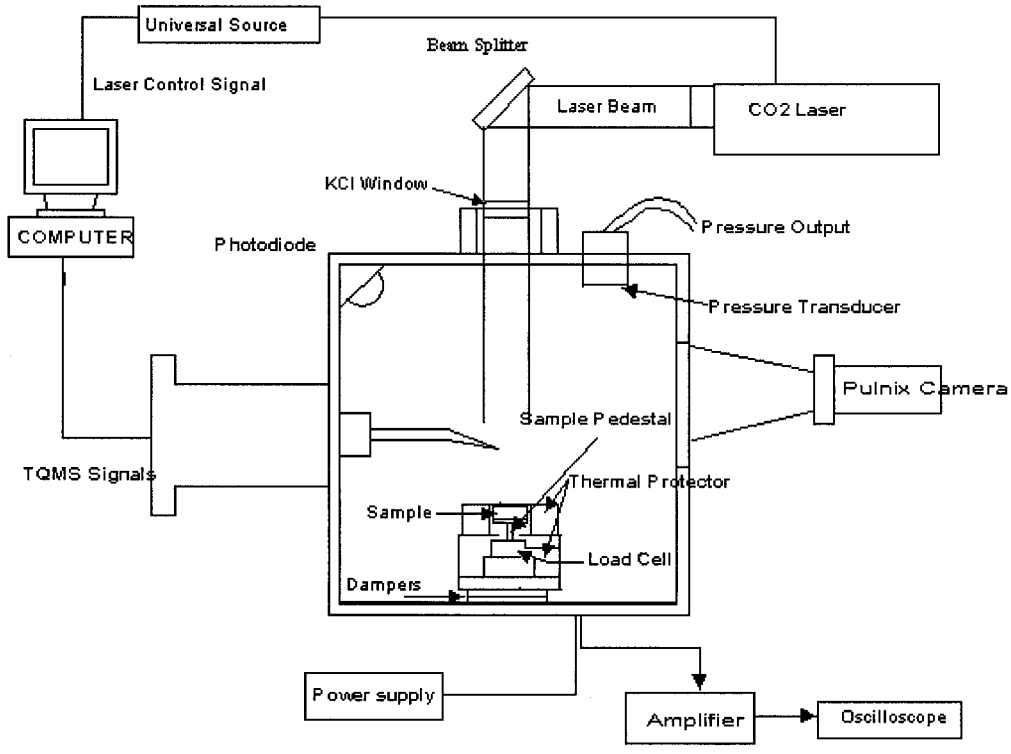

Fig. 2 Schematic of experimental setup for pressure-driven combustion.

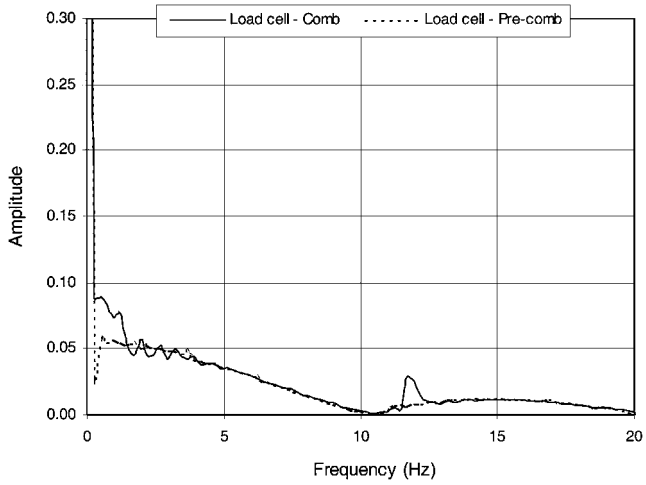

Fig. 3 Fast Fourier transform of the load cell signal before and during combustion.

A DP15TL differential pressure transducer, from Validyne Engineering Corporation, was connected to the chamber. The transducer had one side of its diaphragm exposed to the atmosphere while the other side measured the excitation pressure oscillations produced by the model engines, as well as the change in average chamber pressure. The transducer has a frequency response of greater than 10 kHz. The transducer was connected to a carrier demodulator, Model CD12, which was also from Validyne Engineering Corporation. The demodulator amplified the transducer output and provided the required transducer excitation. The differential output from the demodulator was connected to the two-channel digital oscilloscope.

After a sample was loaded, the chamber was sealed, and the airplane engines were turned on. The resulting load cell signal before combustion was recorded on the digital oscilloscope. A low-pass software filter was used to filter out the high-frequency noise above 500 Hz, and then a fast Fourier transform was performed on these data. Figure 3 shows a typical plot of the fast Fourier transform of the load cell data before and during combustion; these data, at a driving frequency of 12 Hz, were taken during the development of the system using an ammonium perchlorate composite propellant. The amplitude without combustion was subtracted from response amplitude with combustion to obtain the thrust response. During pressure-driven combustion, the ambient pressure rose from its initial value of 1 atm to about 1.5 atm, which further complicated data reduction. As part of the data reduction process, the slow changes in the force and pressure due to combustion of the sample were obtained through a least-squares fit to the data, and they were deleted from the thrust and pressure time traces. Elimination of these slow changes reduced the test-to-test scatter in the amplitude and phase data, especially at low driving frequencies. It also improved the self-consistency of the phase and the overall response function trends in the sense that the phase was consistently positive at frequencies below that of the maximum response. Details of this data reduction procedure may be found in Ref. 18, which is available online, at http://etda.libraries.psu.edu/theses/available/etd-0102101-132547/[August 20, 2002].

Temperature Measurements

To interpret the differences in the pressure- and laser-driven results, the thermal structure of the flames and the heat fluxes from the gas phase to the propellants were needed. Several different types and geometries of fine-wire thermocouples were used to obtain complete temperature profiles from the subsurface to the final flame in the gas phase. For measurements from the subsurface to 0.5 mm above the sample, 25-μm Pt–Pt 13% Rh thermocouples were rolled to a thickness of 10 μm and formed into a U shape to minimize conductive losses. These thermocouples were then inserted between two vertical halves of a cylindrical sample. Measurements from 0.5 mm above the surface through the final flame were made using W/Re thermocouples with bead diameters of 75 μm; the larger bead size was used to extend the life of the thermocouple. The temperature profiles presented are a combination of these measurements, and all are corrected for radiation losses. To get a more consistent measurement of surface temperatures, Pt–Pt 13% Rh thermocouples with a diameter of 25 μm were placed across the propellant surface. The thermocouple wires extended approximately 1 cm beyond the edge of the propellant, and each wire was weighted by small nuts that forced the thermocouple wire to lie on the propellant surface throughout the combustion process.

Results and Discussion

The temperature profiles of the HMX flames are discussed first, so that the results will be available for discussion of the trends in the response data. Following this discussion, the laser- and pressure-driven results are presented and discussed and then compared to the model predictions. Finally, the experimental response amplitudes for laser- and pressure-driven combustion are compared, and key trends are discussed.

Thermal Structure of HMX Flames

Figure 4 shows the temperature profiles for HMX at 35 and 60 W/cm^2 at 1 atm in air. The surface temperatures at 35 and 60 W/cm^2 are 630 ± 10 and 635 ± 10, respectively. The propellant burning rates were 0.54 and 0.72 mm/s. At both incident laser fluxes, the gas-phase temperature shows a very gradual rise in the near-surface region. About 1 mm above the propellant surface, the temperature is 700 K at 60 W/cm^2, whereas at 35 W/cm^2, the temperature 1 mm above the propellant surface is 740 K. At 35 W/cm^2, the temperature profile shows a sharp rise about 1.3 mm above the propellant surface to a final flame temperature of 2100 K. At 60 W/cm^2, the temperature profiles show a sharp rise about 1.5 mm above the propellant surface. These profiles are very consistent with the previous measurements by Tang.[17]

The temperature profiles clearly show that the incident laser flux increases the surface temperature and flame standoff distance above the propellant surface. The near-surface temperature gradients indicate that the gas-phase heat feedback decreases with an increase in heat flux. Other researchers have reported similar effects of laser heating on the structure of nitramine flames at low pressure, for example, see Parr and Hanson-Parr.[19] Note that the flame standoff distance is much larger than that reported by Zenin for HMX self-sustained deflagration at atmospheric pressure in nitrogen.[20] Zenin's results show a final flame position of approximately 0.25 mm, which is substantially less than those observed in the present study. Based on the much larger flame standoff distance compared to the results of Zenin without a laser flux, the heat feedback is expected to be much less than the value of 36 W/cm^2 determined by Zenin. Calculation of the heat feedback based on the temperature gradient in the gas-phase confirmed this expectation; the heat feedback was 3 W/cm^2 at 35 W/cm^2 and 2 W/cm^2 at 60 W/cm^2. Because of the small volume of the pressure-driven test chamber, the mean pressure tended to rise

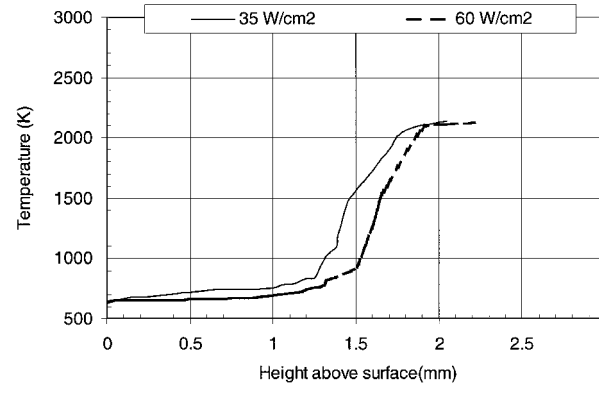

Fig. 4 Temperature profiles for HMX.

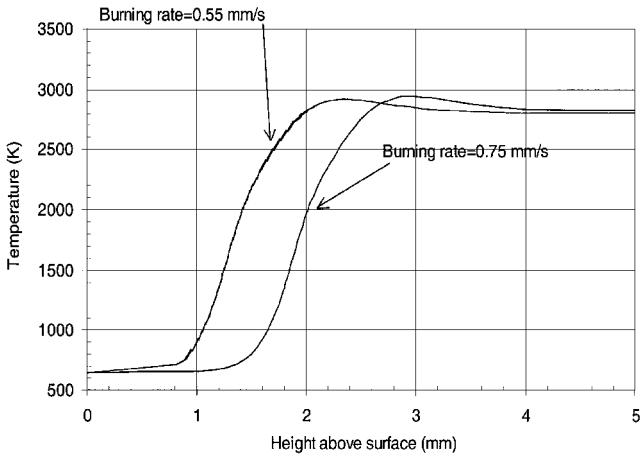

Fig. 5 Modeling predictions of the effect of burning rate on gas-phase temperature profiles.

to approximately 1.5 atm during the test leading to slightly higher burning rates than observed in the laser-driven test chamber. The values of conductive heat feedback estimated from the temperature profiles measured at this pressure were 4 W/cm^2 and 2.5 W/cm^2, at laser fluxes of 35 and 60 W/cm^2, respectively.

To estimate the unsteady component of the heat feedback, the well-established, gas-phase chemistry model for RDX of Yetter et al.[21] was used in the PREMIX model of CHEMKIN. Figure 5 presents typical results for the effect of propellant burning rate on gas-phase temperature profiles. Figure 5 was created using the measured surface temperature, surface species, and burning rate as boundary conditions, with radiation-corrected temperature profiles plus surface and gas-phase species profiles as initial input parameters. The energy equation was solved in the CHEMKIN code, and the resulting temperature profiles are those displayed in Fig. 5. The goal of the modeling was to observe the effect of changing the burning rate, which corresponds to a change in mean heat flux in this study, on near-surface temperature profiles, so that the unsteady component of the heat feedback could be estimated. The model, which assumed no heat losses were present, predicted final temperatures close to the expected value of 3000 K. Because heat feedback from the final flame is not critical in determining the burning rate under the conditions used in this study, the overprediction of the experimental flame temperatures should not introduce significant errors into the estimate of the unsteady heat feedback to the surface. The predicted temperature profiles clearly show that the increase in mass burning rate, corresponding in this case to an increase in heat flux, results in a larger flame standoff distance. The near-surface regions show a gradual temperature rise that is consistent with the experimental measurements.

Laser-Driven Combustion

Figure 6 shows the thrust amplitude and phase responses at heat fluxes of 35 ± 15 and 60 ± 15 W/cm^2. In Fig. 6, 95% confidence intervals based on a minimum of five experiments at each frequency are displayed for response amplitude and phase as error bars. The normalized thrust amplitude is defined as $\Delta\tau/\Delta q$, where $\Delta\tau$ is the thrust amplitude in newtons and Δq is the heat flux amplitude in watts. For both incident heat fluxes, the thrust amplitude is small at low frequency, increases to a peak, and then decreases with an increase in frequency. This trend is consistent with the classical modeling results obtained under the quasi-steady homogeneous one-dimensional framework. At incident heat fluxes of 35 and 60 W/cm^2, the maximum thrust response amplitudes were 0.016 and 0.014 mN/W at driving frequencies of 12 and 16 Hz, respectively. The increase in the mean heat flux results in a lower response amplitude and a higher resonant frequency; this trend has also been observed in the work of Zarko et al.[5,22]

Figure 6b shows the relative phase signal as a function of frequency and heat flux. The phase signal shows a lead at low frequency,

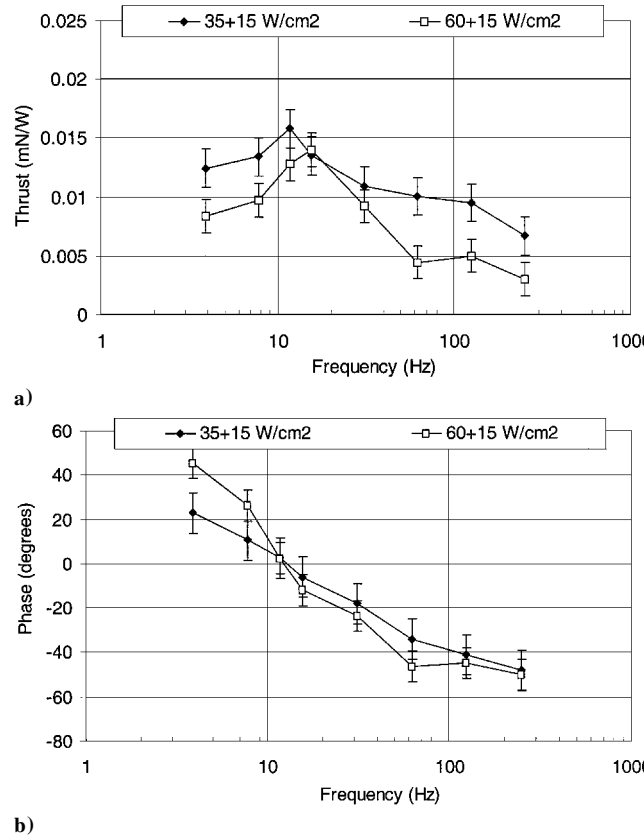

Fig. 6 Thrust amplitude and phase response for laser-driven combustion.

which decreases monotonically to a lag as frequency increases. For an incident heat flux of 35 W/cm^2, the phase signal shows a lead of 21 deg at 4 Hz, zero at 12 Hz, and a lag of 46 deg at 250 Hz. The maximum response amplitude is measured at 12 Hz, and the relative phase at this frequency is zero. The phase and amplitude signals appear to be consistent through the measurements. At 60 W/cm^2, the relative phase leads by 45 deg at 4 Hz, is zero at 16 Hz, and lags by 45 deg at 250 Hz. In general, the trends in the amplitude and phase data are consistent with those reported by Loner and Brewster[11] and Finlinson et al.[23]

An increase in the laser heat flux increases the burning rate and decreases the condensed-phase thermal relaxation time, which can be defined for an opaque material as

$$t_c = \alpha / r_b^2 \tag{1}$$

where r_b is the steady-state propellant surface regression rate and α is the thermal diffusivity. Figure 6a clearly shows that the response amplitude peak shifts to a higher-dimensional frequency with an increase in heat flux and, hence, burning rate. This trend suggests that the response amplitude is related to the condensed-phase thermal relaxation time. To account for the effect of the condensed-phase relaxation time, the response amplitudes are typically plotted against nondimensional frequency. The nondimensional frequency is a product of angular frequency and thermal relaxation time and is given by

$$\Omega = \omega \cdot t_c = 2\pi f \alpha / \bar{r}_b^2 \tag{2}$$

where f is the frequency in hertz.

To facilitate comparison of this response data with the modeling studies, the response amplitude must also be converted into a nondimensional format. The nondimensional form of the response was obtained by perturbing the relationship between average burning rate and thrust given by[3]

$$\bar{\tau} = \bar{m}^2 (RT_f / PM) \tag{3}$$

where $\bar{m}$ is the mean burning rate per unit area, $\bar{\tau}$ is the thrust per unit area, P is the ambient pressure, and M is the average molecular mass. Perturbing Eq. (3) to obtain a relationship between $\Delta m/\bar{m}$ and $\Delta\tau/\bar{\tau}$ and substituting the result into the definition of the laser-driven response function results in the nondimensional laser-driven response given as follows, where $\bar{q}$ is the mean heat flux and Δq is the oscillatory heat flux amplitude:

$$Rq \equiv (\Delta\bar{m}/\bar{m})/(\Delta q/\bar{q}) = (\Delta\tau/\Delta q)(\bar{m}/2\tau)(\bar{q}/\bar{m}) \qquad (4)$$

$\Delta\tau/\Delta q$ and $q/\bar{m}$ in Eq. (4) are obtained through the laser-driven combustion experiments. To determine $\bar{m}/\bar{\tau}$ experimentally, the steady-state burning rate and thrust are required. The signal from the piezoelectric transducer slowly decays over a period of 15 s; hence, a series of square waves were imposed on the HMX pellets to determine the steady-state burn rate and thrust. Figure 7 shows the relationship between surface regression rate and the ratio of regression rate to measured thrust; it shows the trend of decreasing inversely with regression rate, which can be derived in a one-dimensional analysis. As a check on the magnitude of this ratio, it was estimated using an approximate average molecular mass of 26 for the products and the measured flame temperature of 2100 K. The resulting magnitude was 3200 for a regression rate 0.55 mm/s, which is within 15% of the experimental value. Note that this ratio was very challenging to determine experimentally and that it introduces added uncertainty into the response results when they are expressed in dimensionless form.

Figure 8 shows dimensionless R_q as a function of frequency at laser heat fluxes of 35 and 60 W/cm^2; the value of R_q under the limit of $\omega \to 0$ was estimated from the steady-state regression rates to be 0.5. Error bars in this figure 8 and Figs. 9–11 represent 95% confidence intervals. The curves with solid symbols are quasi-steady modeling data obtained from Erikson.[24] The curve without symbols is taken from the work of Loner and Brewster,[11] who presented model prediction only at 35 W/cm^2. The modeling results of

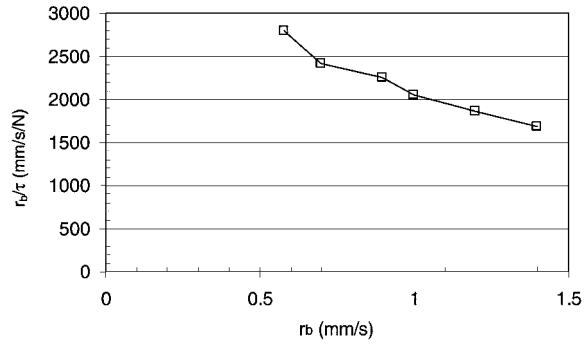

Fig. 7 Relationship between regression rate and ratio of regression rate to thrust.

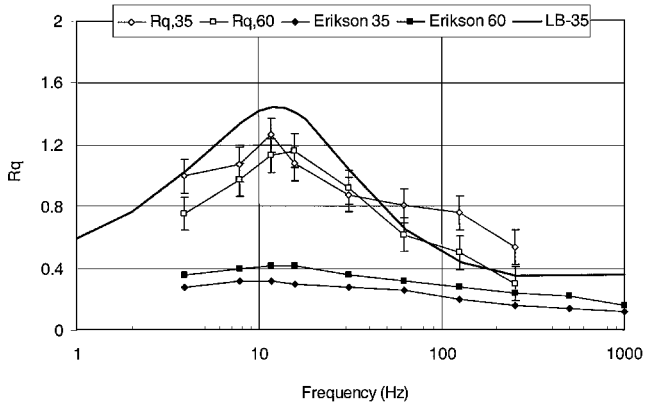

Fig. 8 Comparison of laser-driven response to predictions by Loner and Brewster,[11] Erikson and Beckstead,[13] and Erikson.[24]

Table 1 Total heat flux as a function of unsteady laser-flux during laser-driven combustion

Incident laser flux, W/cm^2	Absorbed laser flux, W/cm^2	Heat feedback, W/cm^2	Net heat flux, W/cm^2
35 ± 15	21 ± 9	3 ± 0.6	24 ± 8.4
60 ± 15	36 ± 9	2 ± 0.5	38 ± 8.5

Erikson and Beckstead[13] predict maximum response function values that are substantially below the measured values; on the other hand, the response function of Loner and Brewster[11] agrees reasonably well with the 35 W/cm^2 data except for the data point at 125 Hz. At the two different heat fluxes, the experimental results have maximum R_q values that are nearly constant at 1.2, whereas the modeling results of Erikson and Beckstead[13] predict an increase in maximum R_q from 0.35 to 0.4 with an increase in laser heat flux. The increase in the maximum nondimensional amplitude response predicted by Erikson[24] is within the experimental uncertainties of this study. Thus, the present study cannot confirm this predicted increase. Erikson[24] believes that the lower values for the response amplitudes obtained by his modeling efforts may be due to inadequate chemical models in the condensed-phase and near-surface gas-phase regions for HMX.

The nearly constant response amplitude with an increase in laser flux from 35 to 60 W/cm^2 can be understood in terms of the net heat flux to the propellant surface and its variation as the laser flux varies. To estimate the variation in the conductive heat feedback, the PREMIX routine of the CHEMKIN code was run at burning rates corresponding to the maximum and minimum amplitudes of the unsteady laser flux. The energy equation was solved for the gas-phase temperature profile, and the estimated values of the gas-phase heat feedback at the two fluxes then gave estimates of the maximum and minimum conductive heat feedback. Table 1 presents the results of these calculations along with the mean and unsteady components of the laser flux, using the estimate of Loner and Brewster[11] that approximately 60% of the incident laser flux is absorbed.

As the laser flux increases, the flame is pushed farther from the sample surface, thereby decreasing the conductive heat feedback. Thus, the unsteady component of the conductive heat feedback will tend to be out of phase with the variation in laser flux. However, for the conditions of these experiments, the unsteady component of the laser flux is much larger than the unsteady component of the heat feedback and, hence, masks the change in heat feedback with laser flux, resulting in the nearly constant response amplitudes observed. In general, the effects of a mean radiant flux on the stability of a flame can be quite complex, sometimes moving a flame from stable to unstable or vice versa, depending on the experimental conditions; see DeLuca et al.[25]

Pressure-Driven Combustion

Thrust response measurements for HMX during pressure-driven combustion were made at 35 and 60 W/cm^2 at frequencies of 4, 8, 12, 16, 32, 64, and 95 Hz. The average burning rates were 0.63 and 0.80 mm/s. As noted earlier, combustion within the small volume of the test chamber for the pressure-driven tests results in a pressure rise from an initial pressure of 1 to about 1.5 atm. As a result, the burning rates are higher than those obtained during laser-driven combustion.

Figure 9 shows the dimensionless thrust amplitude and phase response for HMX at 35 and 60 W/cm^2 during pressure-driven combustion. Substitution of the relationship between $\Delta m/\bar{m}$ and $\Delta\tau/\bar{\tau}$ obtained using Eq. (3) into the definition of dimensionless pressure-driven response function gives

$$Rp \equiv (\Delta\bar{m}/\bar{m})/(\Delta p/\bar{p}) = (\Delta\tau/\Delta p)(\bar{m}/2\tau)(\bar{p}/\bar{m}) \qquad (5)$$

where $\bar{p}$ is the mean pressure and Δp is the amplitude of pressure variation. The data show a low-thrust response at low frequency and then a rise to a peak and decay at the higher frequencies. The resonant peak was observed at a driving frequency of 12 Hz for 35 W/cm^2 and about 16 Hz for 60 W/cm^2; the phase is approximately zero at the maximum amplitude for each set of experiments. The maximum amplitudes were 1.6 at 35 W/cm^2 and 1.4 at 60 W/cm^2. The resonant

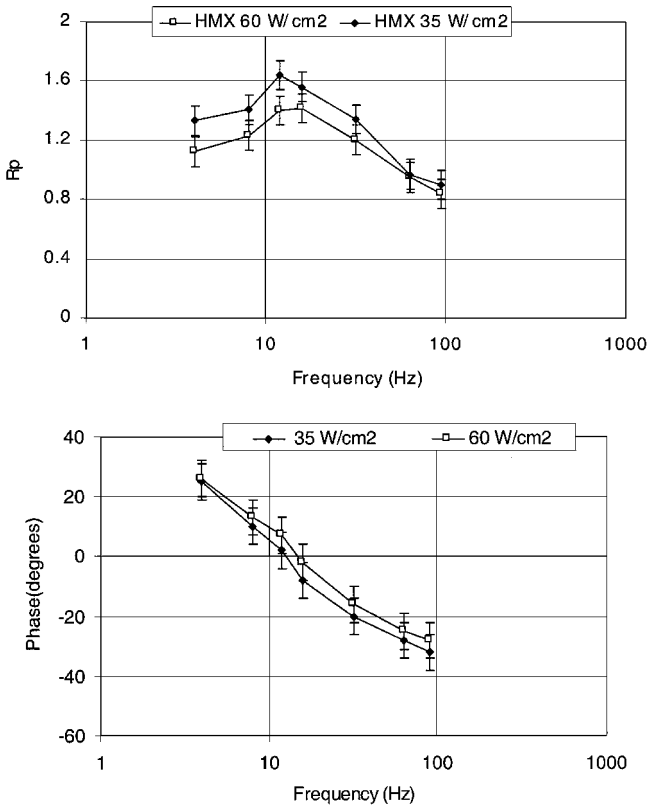

Fig. 9 Dimensionless thrust amplitude and phase response during pressure-driven combustion.

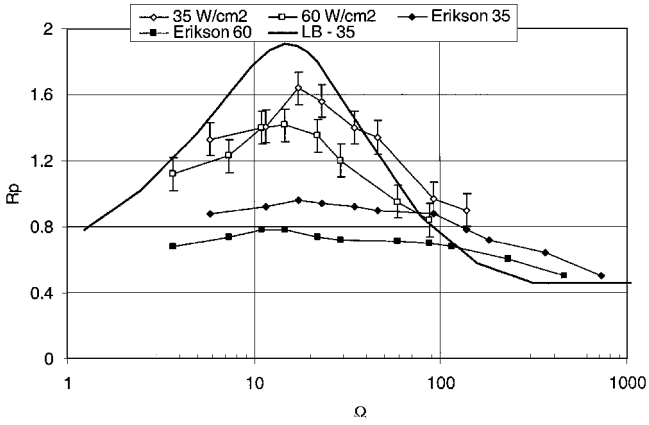

Fig. 10 Comparison of pressure-driven response to predictions by Erikson and Beckstead[13] and Erikson[24] and model of Son and Brewster.[9]

peak is lower and appears to shift to a higher-dimensional frequency with an increase in heat flux. The shift in resonant frequency with the heat flux is consistent with the postulate that the first peak (in this study the only peak) is a result of the condensed-phase thermal relaxation. The values of R_p under the limit of $\omega \to 0$ were determined from the steady-state regression rates to be 0.6 and 0.5 at 35 and 60 W/cm^2, respectively.

Figure 10 shows the thrust response amplitude versus nondimensional frequency for both heat flux cases compared to the modeling results of Erikson and Beckstead[13]; the solid symbols are modeling data obtained from Erikson.[24] Direct comparison to results from Loner and Brewster[11] was not possible as they did not present an R_p prediction. Therefore, their recommended values of the parameters at 35 W/cm^2 were used to generate the pressure-driven response function shown in Fig. 10 based on the model of Son and Brewster.[9] The modeling results of Erikson and Beckstead[13] underpredict the

Table 2 Total heat fluxes as a function of the mean laser-fluxes during pressure-driven combustion

Incident laser flux, W/cm^2	Absorbed laser flux, W/cm^2	Heat feedback, W/cm^2	Net heat flux, W/cm^2
35	21	4 ± 1.3	25 ± 1.3
60	36	2.5 ± 1	38 ± 1

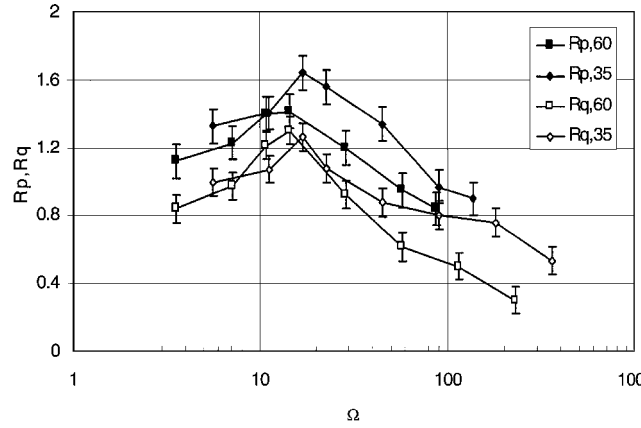

Fig. 11 Comparison of nondimensional thrust response amplitudes during laser- and pressure-driven combustion of HMX.

amplitude of the response, whereas the model of Son and Brewster[9] tends to overpredict the experimental results. Both the models and the experimental data predict the maximum response amplitudes at nondimensional frequencies that lie between 12 and 20. For a change in heat flux from 35 to 60 W/cm^2, the maximum amplitudes decrease from 1.6 to 1.4 in the experiments and from 0.96 to 0.8 in the modeling results of Erikson and Beckstead.[13] Thus, the trends with heat flux are the same between their modeling predictions and the experimental data.

To better understand the effect of the mean laser flux on pressure-driven response amplitudes, the unsteady gas-phase heat feedback was evaluated in the same manner as discussed for the laser-driven tests. Because the pressure-driven response observed is believed to be condensed-phase response to the unsteady gas-phase heat feedback resulting from the oscillatory propellant flames, a decrease in unsteady gas-phase heat feedback with an increase in laser flux should result in a lower response amplitude. The estimated magnitudes for the unsteady heat feedback presented in Table 2 show that the unsteady heat feedback does decrease with an increase in laser flux, consistent with the expected trend.

Comparison Between Laser- and Pressure-Driven Combustion

When the estimated unsteady heat fluxes and the measured thrust response are used, it is possible to calculate the dimensional response in millinewton per watt for the pressure-driven tests. For the peak response at 35 W/cm^2, the pressure-driven data were equivalent to 0.035 mN/W, whereas the peak response of the laser-driven case was 0.016 mN/W based on the nominal heat flux variation of ± 15 W/cm^2. (If the effective absorption coefficient of 0.6 recommended by Loner and Brewster[11] is used, this response would rise to 0.027 mN/W.) That the equivalent pressure-driven response in millinewton per watt is greater than the laser-driven response is consistent with a trend observed by Loner and Brewster. They found that the dimensional response increased as the amplitude of the unsteady flux decreased down to the lowest amplitude at which they could obtain results, ± 9 W/cm^2. In the present study, the estimated unsteady heat fluxes in the pressure-driven tests are much less than those in the laser-driven tests, so the higher response in millinewton per watt for the pressure-driven case is consistent with the Loner and Brewster result.

Figure 11 presents a comparison between non dimensional laser- and pressure-driven combustion response. Whereas the general

trends in the two sets of results are consistent, two differences exist. First, the peak laser-driven response amplitudes do not change with an increase in laser flux, whereas the pressure-driven response amplitudes decrease with an increase in laser flux. In addition, the amplitudes for the laser-driven response are lower than the pressure-driven response amplitudes.

The different behavior of the laser- and pressure-driven combustion response amplitudes with a change in laser flux can be understood by considering the effects of the mean laser flux on gas-phase heat feedback. As discussed earlier, the primary effect of an increase in laser flux is an increase in burning rate and flame standoff distance and a resultant decrease in heat feedback. For the laser-driven tests, the steady gas-phase heat feedbacks are about 3 and 2 W/cm^2 at laser fluxes of 35 and 60 W/cm^2, respectively. During laser-driven combustion, the laser was modulated at amplitudes of ± 15 W/cm^2. Because the unsteady laser flux is much higher than the unsteady gas-phase heat feedback, the laser-driven combustion response measurements are primarily condensed-phase responses to the unsteady laser flux. Because the condensed-phase behavior is not significantly altered by the increase in mean laser heat flux and the unsteady gas-phase heat feedback is overwhelmed by the unsteady laser flux, the condensed-phase response does not change with the increase in mean laser flux during laser-driven combustion. Table 1 shows that there is a very small change in the net unsteady flux that is incident on the propellant surface with the increase in laser flux, resulting in very little change in the propellant response amplitudes.

During pressure-driven combustion, the variation in ambient pressure results in a change in the flame standoff distance and gas-phase heat feedback, causing a variation in the burning rate and resulting thrust, which is measured in this study. The increased laser flux increases the flame standoff distance, decreasing the gas-phase heat feedback and the condensed-phase response amplitudes. Table 2 shows that the mean and unsteady components of the gas-phase heat feedback decrease with the increase in heat flux. Because the propellant condensed phase responds to this unsteady heat feedback, a decrease in this heat feedback results in the lower response amplitude as heat flux increases.

To determine the reasons for the higher response amplitudes during pressure-driven combustion compared to laser-driven combustion, the relationship between thrust and burning rate was examined. The unsteady thrust equation is obtained by perturbing Eq. (3) for mass flux and neglecting the effect of fluctuation in the flame temperature:

$$\Delta\tau = 2\bar{m}\,\Delta m(RT_f/PM) \tag{6}$$

Substitutions for the burning rate, propellant density, and gas density lead to the result

$$\Delta\tau = 2\rho_c \cdot (bp^n) \cdot (n \cdot \Delta p/\bar{p}) \cdot (bp^n)\big/\rho_g \sim p^{2n-1} \tag{7}$$

The overall pressure dependence in Eq. (7) was obtained using $\Delta p/\bar{p}$ being constant for the pressure-driven experiments. Based on this relationship, propellants with a pressure exponent above 0.5 will show larger response amplitudes with an increase in pressure. The pressure exponent of HMX at 1 atm in the absence of a external heat flux is 0.8 (Ref. 26). In the present study, the pressure exponents of the burning rate were estimated to be 0.6 and 0.5 at 35 and 60 W/cm^2. These values would suggest that there should be a greater difference in the pressure- and laser-driven response functions at 35 W/cm^2 than at 60 W/cm^2 and that, at 60 W/cm^2, the two response functions should be nearly the same in magnitude. The results in Fig. 11 are generally consistent with these trends. Hence, the higher response amplitudes during pressure-driven combustion are at least partially due to the increased test pressure of 1.5 atm, compared in the laser-driven tests that were conducted at 1 atm.

Summary

Thrust response data were collected at laser heat fluxes of 35 and 60 W/cm^2 during laser-driven combustion. The dimensional laser-driven response decreased in amplitude and moved to a higher-dimensional frequency with the increase in heat flux. The relationship between burning rate and thrust was used to obtain a nondimensional laser-driven response function that showed that the maximum response amplitude did not change with mean heat flux. The steady-state temperature profiles combined with the pseudounsteady modeling analysis showed that the total unsteady component of the heat flux did not change with the change in mean laser flux. Because the experiments are condensed-phase responses to this unsteady heat flux, the nearly constant values of unsteady heat flux produced the nearly constant laser-driven response amplitudes observed in this study. The analytical response function of Loner and Brewster[11] agrees reasonably well with the experimental results at 35 W/cm^2, whereas the numerical modeling results of Erikson and Beckstead[13] and Erikson[24] predict much smaller amplitudes of the laser-driven response than the experimental results at both heat fluxes.

Pressure-driven thrust response was obtained at mean laser fluxes of 35 and 60 W/cm^2 coupled with peak-to-peak pressure variations of 10%. The nondimensional pressure-driven thrust response decreased in amplitude and shifted to a higher-dimensional frequency with an increase in the laser flux. An analytical pressure-driven response function derived using the work of Son and Brewster[9] and the parameters of Loner and Brewster[11] shows reasonably good agreement to the 35 W/cm^2 data. The modeling results of Erikson and Beckstead[13] and Erikson[24] again underestimate the experimental values, but not by nearly as much as for the laser-driven case. Estimates of the unsteady component of the heat feedback showed that it decreased with an increase in the mean heat flux. Because these experiments were primarily a condensed-phase response to the oscillating propellant flame and, hence, the oscillating gas-phase heat feedback, the decrease in unsteady heat feedback resulted in the lower response amplitudes. In agreement with this trend, the model of Erikson and Beckstead[13] predicts a decrease in maximum response amplitude with an increase in the laser flux.

Acknowledgments

This work was sponsored partly by the Pennsylvania State University and partly by the California Institute of Technology Multidisciplinary University Research Initiative under the Office of Naval Research Grant N00014-95-1-1338, Program Manager Judah Goldwasser. The authors would like to thank M. W. Beckstead, YoungJoo Lee, and Ching-Jen Tang for their insight.

References

[1]Price, E. W., "Solid Rocket Combustion Instability–An American historical Account," *Nonsteady Burning and Combustion Stability of Solid Propellants*," edited by L. DeLuca, E. W. Price, and M. Summerfeld, Progress in Astronautics and Aeronautics Vol. 143, AIAA Washington, DC, 1992, pp. 1–16

[2]Strand, D., and Brown, R. S., "Laboratory Test Methods for Combustion-Stability Properties of Solid Propellants," *Nonsteady Burning and Combustion Stability of Solid Propellants*, edited by L. DeLuca, E. W. Price, and M. Summerfeld, Progress in Astronautics and Aeronautics, Vol. 143, AIAA, Washington, DC, 1992, pp. 519–595.

[3]Mihlfeith, C. M., Baer, A. D., and Ryan, N. W., "Propellant Combustion Instability as Measured by Combustion Recoil," *AIAA Journal*, Vol. 10, No. 10, 1972, pp. 1280–1285.

[4]Simonenko, V. O., Zarko, V. E., and Kutsenogii, K. P., "Experimental Study of the Conditions for Auto- and Forced Fluctuations of the Rate of Combustion of a Powder," *Fzika Goreniya I Vzryva*, Vol. 16, No. 3, 1980, pp. 60–68.

[5]Zarko, V. E., Simonenko, V. N., and Kiskin, A. B., "Radiation-Driven Transient Burning," *Nonsteady Burning and Combustion Stability of Solid Propellants*," L. DeLuca, E. W. Price, and M. Summerfeld, Progress in Astronautics and Aeronautics, Vol. 143, AIAA, Washington, DC, 1992, pp. 363–398.

[6]Brewster, M. Q., Ward, M. J., and Son, S. F., "Unsteady Combustion of Homogeneous Propellants," CPIA Publ. 653, Vol. 2, Chemical Propulsion Information Agency, Laurel, MD, 1996, pp. 181–191.

[7]Tang, C.-J., Kudva, G., Lee, Y., and Litzinger, T. A., "A Study of the Combustion Response of the HMX Monopropellant to Sinusoidal Laser Heating," CPIA Publ. 653, Vol. 2, Chemical Propulsion Information Agency, Laurel, MD, 1996, pp. 159–168.

[8]DeLuca, L., "Theory of Nonsteady Burning and Combustion Stability of Solid Propellants by Flame Models," *Nonsteady Burning and Combustion Stability of Solid Propellants*, edited by L. DeLuca, E. W. Price, and M. Summerfeld, Progress in Astronautics and Aeronautics, Vol. 143, AIAA, Washington, DC, 1992, pp. 519–595.

[9]Son, S. F., and Brewster, W. Q., "Linear Burning Rate Dynamics of Solids Subjected to Pressure or External Radiant Heat Flux Oscillations," *Journal of Propulsion and Power*, Vol. 9, No. 2, 1993, pp. 222–232.

[10]Isbell, R. A., and Brewster, M. Q., "Optical Properties of RDX and HMX," *Materials Research Society Symposium. Proceedings*, Materials Research Society, Pittsburgh, PA, Vol. 418, 1996, pp. 85–90.

[11]Loner, P. S., and Brewster, M. Q., "On the Oscillatory Laser-augmented Combustion of HMX," *Twenty-Seventh Symposium (International) on Combustion*, Combustion Inst., Pittsburgh, PA, 1998, pp. 2309–2317.

[12]Brewster, M. Q., "Solid Propellant Combustion Response, Quasi-Steady (QSHOD) Theory Development and Validation," *Solid Propellant Chemistry, Combustion, and Motor Interior Ballistics*," edited by V. Yang, T. B. Brill, and W.-Z. Ren, Progress in Astronautics and Aeronautics, Vol. 185, AIAA, Reston, VA, 2000, pp. 607–637.

[13]Erikson, W. W., and Beckstead, M. W., "Modeling the Pressure and Heat Flux Responses of Nitramine Propellants with Detailed Kinetics," CPIA Publ. 680, Vol. 1, Chemical Propulsion Information Agency, Laurel, MD, 1998, pp. 415–434.

[14]Lee, Y. J., Tang, C.-J., and Litzinger, T. A., "An Experimental Study of Acoustically-driven Combustion Instabilities of Solid Propellants," CPIA Publ. 662, Vol. 2, Chemical Propulsion Information Agency, Laurel, MD, 1997, pp. 79–91.

[15]Lee, Y. J., Tang, C.-J., and Litzinger, T. A., "Comparison of Laser-driven and Acoustically-driven Combustion of HMX," CPIA Publ. 662, Vol. 2, Chemical Propulsion Information Agency, Laurel, MD, 1997, pp. 253–261.

[16]Lee, Y., Kudva, G., and Litzinger, T. A., "Development of a Facility for Measurement of the Response of Solid Propellants under Pressure-driven Conditions," *Journal of Measurement Science and Technology*, Vol. 11, No. 1, 2000, pp. 51–58.

[17]Tang, C.-J., "A Study of the Steady Chemical Structure of HMX Propellants and Combustion Response to Oscillatory Radiant Heat Flux," Ph.D. Dissertation, Dept. of Mechanical Engineering, Pennsylvania State Univ., University Park, PA, Dec. 1997.

[18]Kudva, G., "A Study of the Laser and Pressure-driven Response Measurements for Solid Propellants at Low Pressure," Ph.D. Dissertation, Dept. of Mechanical and Neuclear Engineering, Pennsylvania State Univ., University Park, PA, Dec. 2000.

[19]Parr, T. P., and Hanson-Parr, D. M., "Solid Propellant Flame Structure," *Materials Research Society Symposium. Proceedings*, Materials Research Society, Pittsburgh, PA, Vol. 418, 1996, pp. 207–219.

[20]Zenin, A., "HMX and RDX: Combustion Mechanism and Influence on Modern Double-Base Propellant Combustion," *Journal of Propulsion and Power*, Vol. 11, No. 4, 1995, pp. 752–758.

[21]Yetter, R. A., Dryer, F. L., Allen, M. T., and Gatto, J. L., "Development of Gas-Phase Reaction Mechanisms for Nitramine Combustion," *Journal of Propulsion and Power*, Vol. 11, No. 4, 1995, pp. 683–697.

[22]Zarko, V. E., Simonenko, V. N., and Kiskin, A. B., "Nonstationary Combustion of Condensed Substances Subjected to Radiation," *Fzika Goreniya I Vzryva*, Vol. 23, No. 5, 1987, pp. 16–26.

[23]Finlinson, J. C., Parr, T., and Hanson-Parr, D., "Laser Recoil, Plume Emission, and Flame Height Combustion Response of HMX and RDX at Atmospheric Pressure," *Twenty-Fifth Symposium (International) on Combustion*, Combustion Inst., Pittsburgh, PA, 1994, pp. 1645–1650.

[24]Erikson, W. W., "Modeling The Unsteady Combustion of Solid Propellants with Detailed Chemistry," Ph.D. Dissertation, Dept. of Chemical Engineering, Brigham Young Univ., Provo, UT, April 1999.

[25]De Luca, L., "Solid Propellant Combustion Response, Quasi-Steady (QSHOD) Theory Development and Validation," *Advances in Combustion Science: In Honor of Ya. B. Zeldovich*, edited by W. A. Sirignano, A. G. Merzhanov, and L. De Luca, Progress in Astronautics and Aeronautics, Vol. 173, AIAA, Reston, VA, 1997, pp. 195–218.

[26]Beckstead, M. W., and Erikson, W. W., "Combustion Instability of Solid Monopropellants," CPIA Publ. 653, Vol. 2, Chemical Propulsion Information Agency, Laurel, MD, 1996, pp. 145–157.